High-performance Ultraviolet Photodetectors Based on ZnO Nanostructures

S. Noothongkaew and O. Thumthan
Department of Physics, Faculty of Science, Ubon Ratchathani University, 34190 Thailand
Email: suttinart_n@yahoo.com

Ki-Seok An
Korea Research Institute Chemical of Technology, Daejeon, 30-5343, South Korea

***Abstract*—Zinc Oxide nanowires were prepared on an Indium Tin Oxide (ITO) substrate by a hydrothermal method which is renowned for its simple, low cost, and low temperature techniques. These wires prepared with different reaction times were demonstrated to be utilized as UV photodetectors. The morphology, elemental compositions, and crystallization of ZnO nanowire structures were analyzed by Field Emission Scanning Electron Microscopy (FE-SEM), X-Ray Spectroscopy (XPS), and X-Ray Diffraction (XRD), respectively. The optical properties of the nanodevices were measured by using UV-vis absorption spectrometer, and the properties of UV photodetectors were characterized by I-V curves. At a given bias voltage of 5 V, ZnO nanowire devices, prepared at the reaction time of 2 h, exhibited high photocurrent, high sensitivity, and fast response time to UV illumination as compared to the devices prepared at the reaction time of 5 h. A higher surface to volume ratio is the main contribution to those properties. These results suggest that the 2-hours ZnO nanowires exhibit great promise for the highly efficient UV photodetectors.**

***Index Terms*—zinc oxide, nanowires, UV-photodetector**

I. Introduction

ZnO is a semiconductor with wide direct band gap energy of 3.35 eV and a large exciton binding energy of 60 meV at room temperature [1]-[3]. It is widely used in optoelectronic devices and microelectronics due to their unique electrical and optical properties. Furthermore, ZnO is easy to prepare with various synthesis methods. ZnO also has lower growth temperature and material cost than other comparable materials. Recently, 1-D ZnO semiconducting nanostructures have been synthesized in various structures such as nanowires, nanorods, nanotubes, and nanobelts. These structures are attracting much attention as very promising candidates for many applications such as UV lasers, light emitting diodes, solar cells, nanogenerators, gas sensors, photodetectors, and photocatalysts [1]-[3]. Among these, ZnO nanowires (ZnO NWs) have attracted intensive research due to the large surface to volume ratio and high aspect ratio. These wires can possess a fast photo response upon illumination of UV light. Thus, it is widely used in ultraviolet (UV) photodectors [4]-[11]. In order to synthesize ZnO nanowires with controlled shape and ordered surface morphology, there has been reported by many different methods such as Vapor Liquid Solid (VLS) [12] and [13], Chemical Vapor Deposition (CVD) [14], Metal Organic Chemical Vapor Deposition (MOCVD) [15], Molecular Beam Epitaxy (MBE) [16], Pulsed Laser Deposition (PLD) [17], and so on. These methods mentioned above are carried out at higher temperatures, high vacuum, and expensive purification processes. Recently, solution phase including chemical bath deposition, (CBD) [18], solvothermal, hydrothermal, self-assembly [19], and sol-gel process have been employed to synthesize ZnO nanowires [20]-[22]. The solution phase method is the simplest, lowest cost, and lowest temperature method compared to those above. This paper focuses on lowcost and low temperature solution- based method for fabrication of UV photodetector with ZnO nanowires and nanorods on ITO substrates by aqueous solution. The advantages of aqueous solution are low cost, simple process, low temperature, and high product yield.

II. Experimental Details

ZnO nanowire arrays were grown on indium thin oxide (ITO) substrate by solution-based technique. The ZnO nanowires were grown on a conductive ITO layer which deposited on a glass substrate with a sheet resistance of 10Ω/cm. The growth of ZnO nanowires were separated into 3 parts. First surface treatment, the cleaned ITO samples were irradiated with oxygen O3 plasma for 5 min in order to seed layer. Second the coating of seed particles, seed solution was prepared by dissolving 0.1-M zinc acetate [Zn(CH3COO)2 ·2H2O] and 10 ml of 2-methoxyethanol as a solvent, and the solution was mixed together in a beaker. This seed solution was spin-coated onto ITO substrate rotated at 2000 rpm for 30 s (3 cycles), and then it was heated at 150 ℃ for 5 min to evaporate the solvent and remove the organic residuals. Finally, growth of ZnO nanowires, the ITO substrate that coated seed solution was put into a growth solution (0.1 M zinc nitrate hydrate, 0.1 M hexamethylenetetramine and 50 ml deionized (DI) water were mixed in beaker) and kept at a temperature of 90 ℃ for 1-5h. After growth, the nanowire

Manuscript received November 27, 2017; revised March 26, 2018.

doi: 10.18178/ijeee.6.1.1-5

ensembles were thoroughly rinsed with DI water and dried in an oven at a temperature of 90 ℃ overnight to reduce the residual contamination on the surface. The morphology and crystal nanostructure of ZnO were characterized by FE-SEM and XRD. Photo-response of ZnO devices were studied by applying a fixed bias voltage and measuring the change in current using a UV light source (Philips TL-D 18W) of power density 350 µWcm-2. Current-voltage (I-V) characteristics of the devices were measured both in the presence and absence of UV light by observing the change in current with the variation in bias voltage from -5 to +5 V.

III. Results and Discussion

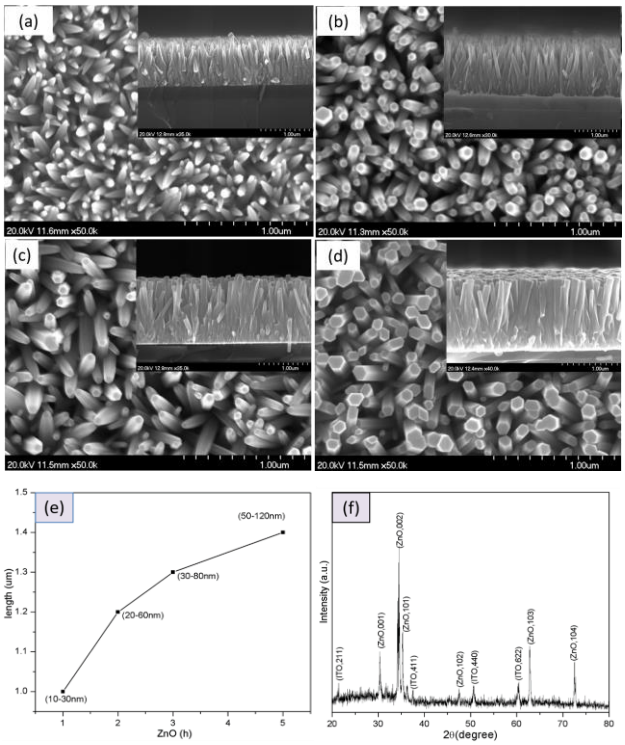

Figure 1. (a-d) the FE-SEM images and cross-section (inset) of ZnO nanowires for 1h, 2h, 3h and 5h, respectively, (e) graph of growth time on x-axis versus length of ZnO on Y-axis, and (f) XRD spectra of ZnO.

The morphology of as grown ZnO nanostructures on indium tin oxide coated glass substrates was examined by using FE-SEM. ZnO nanostructures were prepared with the growth time of 1, 2, 3, and 5h, and the results are shown in Fig. 1(a-d). The ZnO nanostructures had diameters in the range of ~10-30 nm and a length of ~1 µm, for the growth time of 1 h as shown in Fig. 1(a). At the growth time of 2h, the diameter and length were ~ 20-60nm and 1.2 µm, respectively, as observed in Fig. 1(b). After the growth time of 5h, it was clearly observed that the morphology of ZnO nanowires was obtained with a diameter and length in the range of 50-120 nm and 1.4 µm, respectively, as shown in Fig. 1(d). The diameter of the nanowires increased with increasing the growth time. And the nanowires can transform to nanorod-like structures at the growth time of 5h. As the growth duration time increased, the diameter and height of ZnO nanowires increased gradually as shown in Fig. 1(e). This is because more Zn ions were diffused to the ZnO nuclei, thus forming ZnO nanorods [23]. XRD was performed to study the crystal structures of ZnO nanostructures. According to XRD pattern, shown in Fig. 1(f), the diffraction peaks of ZnO nanowires at 2θ are 31.8°, 34.4 °, 36.2 °, 47.5 °, 62.8 °, respectively. All peaks are in good agreement with the standard spectrum (JCPDS nos. 36–1451 and 79–0205) for ZnO [20]-[22]. The high intensity of the (002) peak at 2θ of 34.4° is corresponding to the hexagonal ZnO with wurtzite structure phase in ZnO nanowires. The nanowire structures were grown with highly c-axis oriented on the ITO glass substrate. Impurity peaks were not observed from XRD pattern, indicating that phase-pure and high quality ZnO nanostructures were obtained.

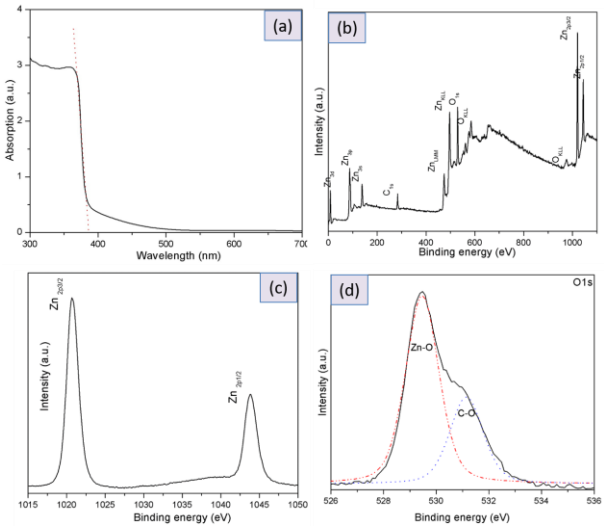

Figure 2. (a) UV-vis absorption, (b) XPS spectrum of the ZnO nanostructures, (c) high resolution of Zn2p, and (d) O1s.

The optical property of pure ZnO nanostructures was determined by UV-vis spectra as shown in Fig. 2(a). The UV absorption appeared from 360 to 400 nm for ZnO nanostructures, corresponding to the promotion of an electron from the valence band to the conduction band. The absorption edge of pure ZnO appears to be about 365 nm which corresponds to the band gap energy of ~3.35 eV at room temperature. The chemical states of the compositional elements in ZnO nanowire structures were characterized by the XPS. The survey XPS spectrum in the Fig. 2(b) shows that the Zn, C, and O peaks with the binding energy of each peak are calibrated by taking the C1s neutral carbon peak at the binding energy of 284.5 eV. XPS spectrum of Zn2p core-level shows double peaks at the binding energy of 1021 and 1044.28 eV corresponding to Zn 2p3/2 and Zn 2p1/2 electrons, respectively, and with spin-orbit splitting at about 23.28 eV as shown in Fig. 2(c). The high and sharp peak at the binding energy of 1021 eV indicates that the Zn 2p3/2 core level is associated with the Zn species in the completely oxidized state. The result of O 1s peak from XPS spectrum is important and interesting because it is not completely symmetrically as shown in Fig. 2(d). And the O1s peak was fitted with two Gaussian peaks. The dominant peak is located at the binding energy of 529.8

eV indicating that O2-ions in the ZnO are hexagonal wurtzite structure. Another peak is located at 531.3 eV corresponding to the adsorbed species containing the C–O bond. Typically, carbon atoms are being contaminated during the preparation process so that it may lead to the bonding of carbon and oxygen atoms.

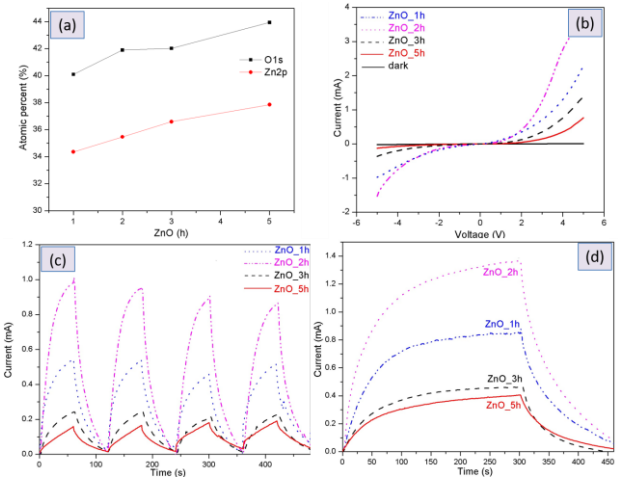

Figure 3. (a) atomic percent of Zn and O elements, (b) I-V characteristics of ZnO nanostructures in dark and under UV illumination, (c) cyclical photoresponses of ZnO devices upon UV illumination with on and off light, (d) saturation current of ZnO nanostructure devices.

Atomic ratio of Zn and O elements was estimated from the XPS results as shown in Fig. 3(a). The average atomic ratio of Zn/O was ~0.86. This result of Zn+2 excessive in the surface while the O2- deficiency may be presented as oxygen vacancy, Zn interstitials, or their complex [24] on the surface. It is able to capture and trap electrons and thus helps in effective photocatalytic degradation of organic pollutants under light irradiation. The I-V characteristic curves of ZnO nanodevices at various reaction times were measured in the dark and under UV light (λ=365 nm) at room temperature as shown in Fig. 3(b-d). All of ZnO nanostructure devices performed in the same conditions under the bias voltage of 5V. For the dark light (black line as shown in Fig. 3(b), it found that the current was about 1.5×10-5 A flowing in the device, corresponding to a resistance of R~3.0×105 Ω at room temperature (I=Iuv-Idark). The depletion layer, formed at the surface of ZnO nanostructure, causes a low dark current because of less charge carrier concentrations. However, the photocurrent slightly increases after the ZnO nanostructure device was exposed to UV light (350 uW/cm-2). It can be seen that the photocurrent of ZnO nanostructure devices at different reaction time were ~2.2×10-3A (1h), ~3.5×10-3 A (2h), ~1.2×10-3 A (3h), and ~6.5×10-3 A (5h), respectively. It is clearly observed that for all of ZnO nanostructure devices, the photocurrent under UV illumination is higher than dark current, indicating that the devices are highly UV sensitive to photoconduction. The photodetectors were also measured with UV light on and off for many cycles with different the reaction times as seen in Fig. 3(c). It indicates that the ZnO nanostructure devices can be reversibly switched between the low and the high conductivity states and shows an excellent stability in each cycle of 2 min. For the growth time of 5 h, it was observed that the current of the device rises rapidly from 0.01×10-3 A to 0.05×10-3 A within 10s and then slowly increases to 0.16×10-3 A (for ZnO 5h). After turn-off the excitation, the photocurrent rapidly decreases within 10s and then slowly decreases to a minimum value. For ZnO nanostructure devices at growth time of 2h, the photocurrent rises instantly from 0.015×10-3 A to 0.44×10-3 A within 10s and then continually increases to 1.0×10-3 A. The photocurrent decreases rapidly within 10s and then slightly decreases to minimum value after turning off the excitation as observed in Fig. 3(c). The results indicate that, the photoresponse of ZnO nanostructure devices at the growth time of 2h is higher than that of ZnO nanostructure devices with 5 h of growth time. According to the results, it can explain the efffects of the size of the ZnO nanorods on the photocurrent. The larger size of nanorods at 5h reduces the surface area which mainly results in a decrease of the photocurrent in response to UV photons due to its relatively low generation of electron-hole pairs [24]. The mechanism of ZnO nanostructure devices was measured in the turn-on/off of UV illumination under the same applied bias voltage that can be described as follows. In the dark, when UV light is turned off, oxygen molecules from ambient air are adsorbed onto the surface of n-type ZnO semiconductor. These oxygen molecules capture free electrons from the surface of ZnO and form negative ion (O_2^-) on the surface of ZnO nanostructure, as shown in the following equation: $O_2(g)+e^- \rightarrow O_2^-(ad)$. This result can cause the formation of a low-conductive depletion layer near the surface of ZnO nanostructures. Under UV light at photon energies above semiconductor band gap, the electron (e-) and hole (e+) pairs are generated. The free electron holes are trapped by adsorbed O_2^- to be desorbed from the surface as defined by the following equation: $h^+ + O_2^-(ad) \rightarrow O_2(g)$. These chemisorption and photodesorption of oxygen molecules from the ZnO surface can result in an increase in the free carrier concentration and a decrease in the width of the depletion layer which lead to an enhancement of carrier injection transport and the higher photocurrent of the ZnO devices [22]. Due to a high surface to volume ratio of ZnO nanowires, it can further enhance the sensitivity of the devices which may lead to the realization of single photon detection. In addition, photoresponse depends on the ambient gas conditions such as it is slowed in vacuum and inert gases (up to several minutes) and fast in ambient air. Fig. 3(d) shows photocurrent saturation as a function of time of ZnO nanodevices at different the growth times of 1h to 5h under bias voltage of 5V. Photocurrent was measured by using UV light exposed to the devices until the photocurrent reaches its maximum value. The results show that photocurrent saturation are 1.4×10-3 A, 8.5×10-4 A, 4.6×10-4 A, and 4.0×10-4 A at reaction time of 2h, 1h, 3h, and 5h, respectively. In addition, the two key parameters, responsivity (Rs) and photocurrent gain (G), of photodetector are important.

The photocurrent saturation of devices was used to calculate the responsivity (Rs) and photocurrent gain (G). These properties were calculated by using the following equation:

$$R_s = \frac{I_{ph}}{A_{area} P_{opt}} = \eta(\frac{q\lambda}{hc})G \quad (1)$$

The photoconductive gain (G) of the detector is defined by the following equation:

$$G = \frac{R_s}{q}\frac{hc}{\lambda} \quad (2)$$

where $I_{ph} = I_{light} - I_{dark}$ is the photocurrent (A), A_{area} is the effective device area (m2), P_{opt} is the incident light power (W/m2), η is the quantum efficiency, h is planck's constant, c is the velocity of the light (m/s), and λ is the wavelength of incident light. The responsivity of ZnO nano-devices with different reaction time are 1.0×104 A/W, 6.7×103 A/W, 3.28×103 A/W, 2.85×103 A/W for 2h, 1h, 3h, and 5h, respectively. The calculated photoconductive gains of ZnO nano-devices are 3.39×104 A/W, 22.7×103 A/W, 11.12×103 A/W, 9.66×103 A/W, for 2h, 1h, 3h, and 5h, respectively. It found that the responsivity and photoconductive gain of ZnO nano-device at the growth time of 2h is high as compared to ZnO nanodevices for 1h, 3h, and 5h. These results can be explained by two reasons. One, because of the morphology of ZnO nano-device at the growth time of 2h shows nanowire-like structure, while ZnO for 5h has a nanorod-like structure. A nanowire-like ZnO has a surface to volume higher than that of a nanorod-like ZnO which may increase the free charge carriers. The other reason is the effect of the lenght of ZnO nanostructures. In this study, it was rationally chosen at the length of 2 μm which is the maximum penetration depth of the incident light in ZnO nanostructures. In addition, further increase in the rod length would increase its electrical resistance which is disadvantage to the enhancement of light capture.

IV. Conlusion

High quality ZnO nanowires were grown on ITO by using a simple, low cost, low temperature, hydrothermal method. Then UV photodetectors were fabricated out of ZnO nanowires with different reaction times. Measurements and analysis showed that the ZnO nano-devices exhibit a high photocurrent under the UV illumination of 365nm at a given bias voltage of 5V. Furthermore, responsivity and photoconductivity gain of ZnO nanostructure devices decreased when the reaction time was increased due to the surface to volume ratio being decreased with the increase in the reaction time. This study suggests the possibility of the promising applications in efficient UV photodetectors.

Acknowledgment

The authors would like to thank National Research Foundation (NRF) for funding support and Korea Research Institute of Chemical Technology, (KRIC), South Korea for experiment support facilities and Ubon Ratchathani University for allowing in this research.

References

[1] Y. Jin, J. Wang, B. Sun, J. C. Blakesley, and N. C. Greenham, "Solution processed ultraviolet photodetectors based on colloidal ZnO nanoparticles," *Nano Letters*, vol. 8, no. 6, pp. 1649-1653, 2008.

[2] Y. Zhang, M. K. Ram, and E. K. Stefanakos, "Synthesis characterization and applications of ZnO nanowires," *J. of Nanomaterials*, pp. 624520-22, 2012.

[3] S. Noothongkaew, S. Pukird, and K. S. An, "Synthesis of zinc oxide nanowire-nanowall-like hybrid structures on graphene," *Integrated Ferroelectrics*, vol. 165, pp. 146–152, 2015.

[4] B. D. Boruan, D. B. Ferry, A. Mukherjee, and A. Misra, "Few layer graphene/ZnO nanowires based high performance UV photodetector," *Nanotechnology*, vol. 26, p. 235703, 2015.

[5] R. K. Biroju, N. Tilak, and G. Rajender, "Catalyst free growth of ZnO nanowires on graphene and graphene oxide and its enhanced photoluminescence and photoresponse," *Nanotechnology*, vol. 26, p. 145601, 2015.

[6] M. S. Akhtar, J. H. Hyung, D. J. Kim, T. H. Kim, and S. K. Lee, "A comparative photovoltaic study of perforated ZnO nanotube/TiO_2 thin film and ZnO nanawire/TiO_2 thin film electrode-based dye-sensitized solar cells," *J. of the Korea Physical Society*, vol. 56, pp. 813-817, 2010.

[7] H. Zhang, A. V. Babichev, G. Jacopin, P. Lavensus, and F. H. Julien, "Characterization and modeling of a ZnO nanowire ultraviolet photodetector with graphene transparent contact," *J. of Applied Physics*, vol. 114, p. 234505, 2013.

[8] K. J. Chen, F. Y. Hung, S. J. Chang, and S. J. Young, "Optoelectronic characteristics of UV photodetector based on ZnO nanowire thin films," *J. of Allows and Compounds*, vol. 479, pp. 674-677, 2009.

[9] Q. Yang, X. Guo, W. Wang, Y. Zhang, and S. Xu, "Enhancing sensitivity of a single ZnO micro- /nanowire photodetector by piezo-phototronic effect," *ACS Nano*, vol. 4, no. 10, pp. 6285–6291, 2010.

[10] C. Soci, A. Zhang, B. Xiang, and S. A. Dayeh, "ZnO nanowire UV photodetectors with high internal gain," *Nano Letters*, vo.l. 7, pp. 1003-1009, 2007.

[11] H. Zeng, Y. Cao, S. Xie, J. Yang, Z. Tang, and X. Wang, "Synthesis optical and electrochemical properties of ZnO nanowires/graphene oxide heterostructures," *Nanoscale Research Letters*, vol. 8, p. 133, 2013.

[12] L. N. Protasova, E. V. Rebrov, and K. L. Choy., "ZnO based nanowires grown by chemical vapour deposition for selective hydrogenation of acetylene alcohols," *Catalysis Science and Technology*, vol. 1, pp. 768-777, 2011.

[13] D. Wu, Y. Jiang, Y. Zhang, and J. Li., "Device structure-dependent field effect and photoresponse performances of p-type ZnTe:Sb nanoribbons," *J. Mater. Chem.*, vol. 22, p. 6206, 2012.

[14] S. Ashraf, A. C. Jones, and J. Bacsa, "MOCVD of vertically aligned ZnO nanowires using bidentate ether adducts of dimethylzinc," *Chemical Vapor Deposititon*, vol. 17, pp. 45-53, 2011.

[15] L. Wang, X. Zhang, S. Zhao, G. Zhou, Y. Zhou, and J. Qi., "Synthesis of well-aligned ZnO nanowires by simple physical vapor deposition on c-oriented ZnO thin films without catalysts or additives," *Applied Physics Letters*, vol. 86, p. 024108, 2005.

[16] J. S. Wang, C. S. Yang, and P. I. Chen., "Catalyst-free highly vertically aligned ZnO nanoneedle arrays grown by plasma-assisted molecular beam epitaxy," *Applied Physics A*, vol. 97, pp. 553-557, 2009.

[17] L. C. Tien, S. J. Pearton, D. P. Norton, and F. Ren., "Synthesis and microstructure of vertically aligned ZnO nanowires grown by high-pressure-assisted pulsed-laser deposition," *Journal of Materials Science*, vol. 43, pp. 6925-6932, 2008.
[18] L. K. Krasteva, K. I. Papazova, A. S. Bojinova, and N. V. Kaneva, "Synthesis and characterization of ZnO and TiO_2 powders, nanowire ZnO and TiO_2/ZnO thin films for photocatalyc applications," vol. 45, pp. 625-630, 2013.
[19] M. Y. Guo, M. K. Fung, F. Fang, and X. Y. Chen, "ZnO and TiO_2 1D nanostructures for photocatalytic applications," *J. of Alloys and Compounds*, vol. 509, pp. 1328-1332, 2011.
[20] S. Lib, Y. S. Chu, D. Z. Shen, Y. M. Lu, and Y. J. Zhang, "High quality ZnO thin films grown," *Journal of Applied Physics*, vol. 91, pp. 501-505, 2002.
[21] K. Uma, S. Ananthakumar, R. V. Mangalaraja, T. Soga, and T. Jimbo, "Growth and improvement of ZnO nanostructure using aged solution by flow coating process," *Advances in Materials Physics and Chemistry*, vol. 3, pp. 194-200, 2013.
[22] H. Kind, H. Yan, B. Messer, M. Law, and P. Yang, "Nanowire ultraviolet photodetectors and optical switches," *Adv. Mater*., vol. 14, no. 2, pp. 158-160, 2002.
[23] Y. H. Ko, G. Nagaraju, and J. S. Yu, "Fabrication and optimization of vertically aligned ZnO nanorods array based UV photodetectors via selective hydrothermal synthesis," *Nanoscale Research Letters*, vol. 10, p. 323, 2015.
[24] J. Zhang, D. Gao, and G. Yang, "Synthesis and magnetic properties of Zr dopedZnO nanoparticles," *Nanoscale Research Letters*, vol. 6, pp. 587-593, 2011.

Asst. Prof. Dr. Suttinart Noothongkaew is with Faculty of Science Ubon Ratchathani University 85 Sathollmark Rd. Warinchamrab Ubon Ratchathani, Thailand 34190.

Her Education: 2006-2011, Doctor of Philosophy in Physics Dissertation in In-situ Photoemission study of ZnO formed by thermal oxidation; 2002-2005: Master of Science (Major in Applied Physics) King Mongkut's Institute of Technology Ladkrabang Bangkok Thailand; 1996-2000: Bachelor of Science (Major in Physics) Ramkhumhang University, Thailand.

Her working experience: Researcher at High Energy Accelerator Research Organization (KEK), 1-1 Oho, Tsukuba-Shi, Ibaraki-ken, 305-0801, Japan. I worked in Magnetic Circular Dichroism (MCD) of Ni sample with UV-PEEM. To gain knowledge and experience in the area of PEEM technique (May 2009 – Nov 2009); Korea Research Institute of Chemical Technology (KRICT), Deajeon, South Korea. I worked in ZnO nanostructures on Graphene (March 2013-May 2013); Visiting research in ferromagnetic materials at Synchrotron Light Research Institute, SLRI, Nakhon-Ratchasima, Thailand (March 2014 – April 2014); Visiting research in Graphene Oxide (GO) and reduced Graphene Oxide (rGO), at Korea Research Institute of Chemical Technology, KRICT, South Korea (June 2014 – July 2014); Postdoctoral Fellowship in Metal oxide, Semiconductor and nanostructures, at Korea Research Institute of Chemical Technology, KRICT, South Korea (July 2015-July 2016).